Josephson Effect between two weakly-interacting Bose-Einstein Condensates

Author: Martí Cladera Rosselló
Facultat de Física, Universitat de Barcelona, Diagonal 645, 08028 Barcelona, Spain.

Advisor: Montserrat Guilleumas Morell

Abstract: In this work, we study the Josephson dynamics, a coherent tunneling of particles between two Bose-Einstein condensates, spatially confined in a double-well potential, at zero temperature. We have derived the dynamical equations of our system by using the Gross-Pitaevskii equation as theoretical framework, together with a two-mode approximation. We have investigated the tunneling dynamics within the Standard Two-Mode model, neglecting the overlap of nonlinear interaction terms, as well as within the Improved Two-Mode approximation, without neglecting them. We have obtained the interaction ranges where the Improved Two-Mode is necessary in order to accurately describe the dynamics of the system.

I. INTRODUCTION

In 1924, Albert Einstein, following the research done by Satyendra Nath Bose's paper on quantum statistics, predicted a new state of matter: the Bose-Einstein condensate (BEC). It is formed when a spatially restricted dilute gas of bosons is cooled down to temperatures of the order of nanokelvin (nK) [1]. Bosons, unlike fermions, are particles that can occupy the same single-particle quantum state due to the symmetry under permutations in their wave function. This symmetry produces the absence of the Pauli exclusion principle. At extremely low temperatures, a considerably large fraction of bosons occupy the lowest energy single-particle state. The de Broglie wavelength of the particles depends on the temperature as $\lambda \propto T^{-1/2}$. When $T \to 0$, the average distance between the particles and the wavelengths of this particles overlap losing their particle identity, and generating a matter wave. This phenomenon gives rise to a unique coherent macroscopic entity, which can be described by a single-particle wave function. This system allows quantum properties to become apparent on a macroscopic scale, the BEC.

The Josephson effect [2] is going to be the subject of our study. It is a quantum phenomenon, first predicted in superconductors by Brian David Josephson in 1962. It corresponds to a a coherent flow of Cooper pairs (pairs of electrons), which are bosonic in nature, tunneling through a barrier in the presence of a chemical potential gradient. The first experimental observation of the Josephson effect was in 1963, and it is attributed to P.W. Anderson and J.M. Rowell. In superconductors, the two interacting systems are separated by a thin insulating layer [3]. Josephson effect has also been experimentally observed between two weakly-interacting BECs [4]. In our study, a double-well symmetric potential plays the role of the thin insulator or barrier. The external potential also acts as a trap in order to confine the bosons, enabling the condensation of the boson gas in both wells, when the system is cooled down to $T \simeq 0$.

The Two-Mode (TM) approximation enables the study of the dynamics of the system as if there were two trapped condensates, one on each side of the well [5]. There are two kinds of TM approximations: the Improved Two-Mode (I2M) approximation [6], which takes into account the overlap of the left and right wave functions, and The Standard Two-Mode (S2M) approximation [7], which neglects the overlap. We will investigate the tunneling dynamics and the different regimes in both approximations, as well as in which regime the I2M is necessary when studying the tunnelling between two weakly-linked BEC.

II. THEORETICAL FRAMEWORK

A. The Gross-Pitaevskii equation

We use the Gross-Pitaevskii (GP) equation as our theoretical framework. It is a non-linear Schrödinger-like equation and has the form of a mean-field equation. This framework provides good results when the number of bosonic particles, N, is large enough so that quantum fluctuations can be neglected, temperature is sufficiently low, and the system is weakly interacting.

The many-body Hamiltonian of a system of N weakly interacting bosons trapped in an external potential, $V_{\text{ext}}(\mathbf{r})$, in the limit of low temperature, $T \simeq 0$, can be written as:

$$\mathcal{H} = \sum_{i=1}^{N} \left(-\frac{\hbar^2}{2m}\nabla_i^2 + V_{\text{ext}}(\mathbf{r}_i) \right) + g \sum_{i<j} \delta(\mathbf{r}_i - \mathbf{r}_j)\,, \quad (1)$$

where we have considered contact interacting particles. Here $g = 4\pi\hbar^2 a_s/m$ is the coupling constant, which acts as an effective atomic interaction, and is proportional to the s-wave scattering length, a_s. From Eq. (1), it follows the energy functional.

$$\mathcal{E} = N \int d^3\mathbf{r} \left(\frac{\hbar^2}{2m}|\nabla\Phi(\mathbf{r})|^2 + V_{\text{ext}}(\mathbf{r})|\Phi(\mathbf{r})|^2 + \frac{gN}{2}|\Phi(\mathbf{r})|^4 \right). \quad (2)$$

By minimizing (2) under variations of Φ, with the normalization constraint, $\int \mathrm{d}^3\,\mathbf{r}\,|\Phi(\mathbf{r})|^2 = 1$, it follows the time-dependent GP equation [2]:

$$i\hbar\frac{\partial}{\partial t}\Psi(\mathbf{r}) = \left(-\frac{\hbar^2}{2m}\nabla^2 + V_{\text{ext}}(\mathbf{r}) + g|\Psi(\mathbf{r})|^2 \right) \Psi(\mathbf{r})\,, \quad (3)$$

where now, for convenience, we have used $\Psi = \sqrt{N}\Phi$.

B. Two-mode approximation

We consider two weakly-interacting BECs at $T \simeq 0$. The system is confined by a double-well symmetric potential, which ensures a weak link while allowing tunneling between the two sides. This confining potential can be obtained by the combination of a centered Gaussian barrier, and an harmonic potential with trapping frequency ω [8]: $V_{\text{ext}} = \frac{1}{2}r^2 + V_b e^{-\frac{r^2}{2}}$, where V_b is the height of the barrier. Dimensionless units are assumed, the distances are scaled by $\sqrt{\hbar/(m\omega)}$, and energies by $\hbar\omega$.

When the overlap between the left and right component of the system is small, the total wave function can be expressed as the superposition of two time-independent spatial wave functions $\Phi_L(\mathbf{r})$ and $\Phi_R(\mathbf{r})$, mostly localized on the left and right well, respectively. Both wave functions are normalized in unity. In the mean-field approximation, in presence of a weak link, the total wave function can be written as: $\Psi(\mathbf{r},t) = \Psi(\mathbf{r},t)_L + \Psi(\mathbf{r},t)_R$, referring to the the left and right condensates wave functions. This yields the two-mode ansatz [2, 7]:

$$\Psi(\mathbf{r},t) = \psi_L(t)\Phi_L(\mathbf{r}) + \psi_R(t)\Phi_R(\mathbf{r})\,. \tag{4}$$

This wave function is normalized to N. The spatially localized wave functions $\Phi_{L(R)}(\mathbf{r})$ can be constructed from the linear combination of the ground state and the first excited state of the double-well potential [7].

Due to the coherence properties of a BEC [2], one can define $\psi_j(t) = \sqrt{N_j(t)}e^{i\phi_j(t)}$, where $\phi_j(t)$ is the phase of the wave function, and $N_j(t)$ the number of particles in the left ($j = L$) or right ($j = R$) well. The total number of particles, $N = N_L + N_R$, is constant.

Inserting (4) into the time-dependent GP Eq. (3), one obtains a system of coupled equations. Since $\Phi_L(\mathbf{r})$ and $\Phi_R(\mathbf{r})$ are weakly linked, one can, in first approximation, neglect the overlap of high-order mixed products between Φ_R and Φ_L (nonlinear interaction terms), obtaining the so-called S2M approximation [5, 7]:

$$\begin{cases} i\hbar\dfrac{\partial\psi_L(t)}{\partial t} = \left[\varepsilon + \mathcal{U}\cdot N_L\right]\psi_L(t) - \mathcal{K}\psi_R(t) \\ i\hbar\dfrac{\partial\psi_R(t)}{\partial t} = \left[\varepsilon + \mathcal{U}\cdot N_R\right]\psi_R(t) - \mathcal{K}\psi_L(t)\,, \end{cases} \tag{5}$$

where we have defined:

$$\begin{gathered} \varepsilon_i = \int d^3\mathbf{r}\left[\frac{\hbar^2}{2m}|\nabla\Phi_i(\mathbf{r})|^2 + |\Phi_i(\mathbf{r})|^2 V_{\text{ext}}(\mathbf{r})\right], \\ \mathcal{K} = -\int d^3\mathbf{r}\left[\frac{\hbar^2}{2m}\nabla\Phi_i(\mathbf{r})\nabla\Phi_j(\mathbf{r}) + \Phi_i(\mathbf{r})V_{\text{ext}}(\mathbf{r})\Phi_j(\mathbf{r})\right], \\ \mathcal{U}_i = g\int d^3\mathbf{r}\ |\Phi_i(\mathbf{r})|^4. \end{gathered} \tag{6}$$

In this paper, we will also study the case where the interaction integrals involving high-order mixed products are not neglected. This model is called the I2M approximation. Analogously to Eqs. (5) one obtains the I2M equations taking into account the overlapping nonlinear interaction terms [6]:

$$\begin{cases} i\hbar\dfrac{\partial\psi_L(t)}{\partial t} = \left[\varepsilon + \mathcal{U}\cdot N_L\right]\psi_L(t) - \mathcal{K}\psi_R(t), \\ \quad +\mathcal{I}\left[N_R\psi_L(t) + (\psi_L^*(t)\psi_R(t) + \psi_L(t)\psi_R^*(t))\cdot\psi_R(t)\right], \\ \quad -\mathcal{F}\left[N\psi_R(t) + (\psi_L^*(t)\psi_R(t) + \psi_L(t)\psi_R^*(t))\cdot\psi_L(t)\right]. \\ i\hbar\dfrac{\partial\psi_R(t)}{\partial t} = \left[\varepsilon + \mathcal{U}\cdot N_R\right]\psi_R(t) - \mathcal{K}\psi_L(t), \\ \quad +\mathcal{I}\left[N_L\psi_R(t) + (\psi_R^*(t)\psi_L(t) + \psi_R(t)\psi_L^*(t))\cdot\psi_L(t)\right], \\ \quad -\mathcal{F}\left[N\psi_L(t) + (\psi_R^*(t)\psi_L(t) + \psi_R(t)\psi_L^*(t))\cdot\psi_R(t)\right], \end{cases} \tag{7}$$

where $\mathcal{F}$ and $\mathcal{I}$ are defined as:

$$\begin{aligned} \mathcal{F}_i &= -g\int d^3\mathbf{r}\ \Phi_i^3(\mathbf{r})\Phi_j(\mathbf{r}), \\ \mathcal{I} &= g\int d^3\mathbf{r}\ |\Phi_i(\mathbf{r})|^2|\Phi_j(\mathbf{r})|^2. \end{aligned} \tag{8}$$

Since V_{ext} is symmetric, the parameters in (6) and (8) are independent of whether the condensate is confined in the left or right well, $i = L, R$.

Both S2M and I2M approximations can be solved numerically, Eq. (5) and (7), respectively. However, expressing these equations in terms of two new variables: the population imbalance, $z(t)$, and the phase difference between the right and left side of the potential barrier, $\delta\phi(t)$, make some physical features emerge more naturally:

$$z(t) = \frac{N_L - N_R}{N}, \quad \delta\phi(t) = \phi_R(t) - \phi_L(t)\,. \tag{9}$$

Rewriting (5) and (7) in terms of these new variables, and expressing the time in units of the corresponding Rabi frequency, $\omega_R^{\text{S2M}} = 2\mathcal{K}/\hbar$ and $\omega_R^{\text{I2M}} = 2(\mathcal{K} + \mathcal{F}N)/\hbar$, one arrives at the following dimensionless systems of two non-linear coupled equations for the S2M and I2M, respectively:

$$\begin{cases} \dfrac{\partial z(t)}{\partial t} = -\sqrt{1 - z^2(t)}\sin\delta\phi(t), \\ \dfrac{\partial\delta\phi(t)}{\partial t} = \Lambda z(t) + \dfrac{z(t)}{\sqrt{1 - z^2(t)}}\cos\delta\phi(t). \end{cases} \tag{10}$$

$$\begin{cases} \dfrac{\partial z(t)}{\partial t} = -\sqrt{1 - z^2(t)}\sin\delta\phi(t) + \zeta(1 - z^2)\sin 2\delta\phi, \\ \dfrac{\partial\delta\phi(t)}{\partial t} = \tilde{\Lambda} z(t) + \dfrac{z(t)}{\sqrt{1 - z^2(t)}}\cos\delta\phi(t) - \zeta z(2 + \cos 2\delta\phi). \end{cases} \tag{11}$$

The parameters Λ and $\tilde{\Lambda}$ are dimensionless and quantify the strength of the mean-field interactions. They are defined as:

$$\Lambda = \frac{N\mathcal{U}}{\hbar\,\omega_R^{\text{S2M}}} \ ; \ \tilde{\Lambda} = \frac{N\mathcal{U}}{\hbar\,\omega_R^{\text{I2M}}}\,. \tag{12}$$

The parameter ζ is defined as: $\zeta = N\mathcal{I}/2(\mathcal{K} + \mathcal{F}N)$. Notice that it arises in the I2M, when the mixed overlap products integrals are not negligible. Indeed, when

$\mathcal{F} = \mathcal{I} = 0$, hence, $\zeta = 0$, one returns to the S2M equations (10).

Analogously, from the density functional (2), one can derive the Hamiltonian of the system. Notice that the Hamiltonian for I2M is not the same as for S2M:

$$\mathcal{H}_{\text{S2M}}(z, \delta\phi) = \frac{\Lambda}{2} z^2(t) - \sqrt{1 - z^2(t)} \cos \delta\phi(t) \,, \qquad (13)$$

$$\mathcal{H}_{\text{I2M}}(z, \delta\phi) = \frac{\tilde{\Lambda}}{2} z^2 - \sqrt{1 - z^2} \cos \delta\phi + \frac{\zeta}{2}(1 - z^2)(2 + \cos 2\delta\phi) \,. \qquad (14)$$

The variables $z(t)$ and $\delta\phi(t)$ behave as canonical conjugate variables:

$$\dot{z}(t) = -\frac{\partial \mathcal{H}_\alpha}{\partial \delta\phi} \,; \quad \delta\dot{\phi}(t) = \frac{\partial \mathcal{H}_\alpha}{\partial z} \qquad \alpha = \{\text{S2M,I2M}\}, \qquad (15)$$

with them one recovers Eqs. (10) and (11). These systems can be solved when a set of initial values for the population imbalance, $z_0 \equiv z(0)$, and phase difference, $\delta\phi_0 \equiv \delta\phi(0)$, is provided.

C. Dynamical regimes

Our system yields two distinct dynamical behaviours conditioned by the strength of the interaction, Λ or $\tilde{\Lambda}$, for the S2M and I2M respectively, and the initial conditions. These regimes are the Josephson effect (JE) regime and the Macroscopic Quantum Self-Trapping (MQST) regime.

Josephson dynamics is characterized by a fast oscillating tunneling of population (bosons) crossing across the potential barrier, in our case it is symmetrical and high enough to secure a weakly-linked system, but not as high to have two independent and non-interacting BEC.

The system, when in Josephson's regime, evolves following closed trajectories in the $(z, \delta\phi)$ plane, around either a maximum or a minimum point of the system. In addition, the JE is characterized by a mean population imbalance over time equal to zero, $\langle z \rangle_t = 0$.

On the other hand, MQST occurs when tunneling is strongly suppressed, confining a great fraction of particles in one side of the well. In this regime, the oscillations yield $\langle z \rangle_t \neq 0$. Additionally, another feature of MQST is that the population imbalance does not change sign during the evolution. MQST occurs due to the nonlinearity of the GP equation.

It is possible to analytically find the critical value of both Λ and $\tilde{\Lambda}$, where the transition between the JE and MQST regimes occur, imposing that the corresponding Hamiltonian, Eqs. (13) and (14), has to be equal or greater than $\mathcal{H}_\alpha(0, \pi)$, with $\alpha = \{\text{S2M,I2M}\}$ [5]. Below the critical value JE dominates, contrarily, when the critical value is surpassed, MQST reigns. The critical values of the interaction parameters are:

$$\Lambda_c = \frac{1 + \sqrt{1 - z_0^2} \cos \delta\phi_0}{z_0^2/2} \,, \qquad (16)$$

$$\tilde{\Lambda}_c = \Lambda_c + \frac{\zeta}{z_0^2} \left[3 - (1 - z_0^2)(2 + \cos 2\delta\phi_0)\right] \,. \qquad (17)$$

For non-zero values of ζ, the additional term in (17) is always greater than zero. This means that when taking into account the nonlinear interaction terms (I2M), the region of oscillating tunneling around $z = 0$ is larger, hence, the Josephson domain is enhanced.

III. NUMERICAL RESULTS

Our study will be based on the parameters extracted from Refs. [6, 9]. Furthermore, in Sect. III A, we are going to use $(z_0 = 0.8, \delta\phi_0 = \pi)$ as our initial conditions, hence, we find different $\tilde{\Lambda}_c$ depending on the used parameters:

- From [6]: $N = 10^5$, $\mathcal{K} = 1.2915 \times 10^{-3}\hbar\omega$, $\mathcal{F} = 2.0245 \times 10^{-8}\hbar\omega$, and $\mathcal{I} = 3.9960 \times 10^{-10}\hbar\omega$. So, $\zeta = 0.0068$, and $\Lambda_c = 1.25$, $\tilde{\Lambda}_c = 1.27$.
- From [9]: $N = 1150$, $\mathcal{K} = 1.89 \times 10^{-2}\hbar\omega$, $\mathcal{F}N = 2.51 \times 10^{-2}\hbar\omega$, and $\mathcal{I}N = 5.62 \times 10^{-3}\hbar\omega$. So, $\zeta = 0.06$, and $\Lambda_c = 1.25$, $\tilde{\Lambda}_c = 1.43$.

A. Population imbalance evolution

We have obtained the dynamical evolution by solving the differential equations (10) and (11), S2M and I2M respectively, by using a Runge-Kutta method of order 4. We have used a fixed set of initial values, and a certain value of the interaction parameter, Λ_0 (numerical value of Λ and $\tilde{\Lambda}$ used to solve the differential equations).

When $\Lambda_0 \notin [\Lambda_c, \tilde{\Lambda}_c]$, where tunneling is strongly suppressed, both I2M and S2M yield the same qualitative results. In some cases, e.g. see Fig. 1, even the quantitative results from both approximations are roughly equal. In this figure, the value of Λ_0 is greater than $\tilde{\Lambda}_c$. Consequently, the characteristic periodic oscillations around $z \neq 0$, without a sign change in $z(t)$, that corresponds to a MQST regime can be observed. If $\Lambda_0 < \Lambda_c$ one would observe a behaviour corresponding to a JE regime.

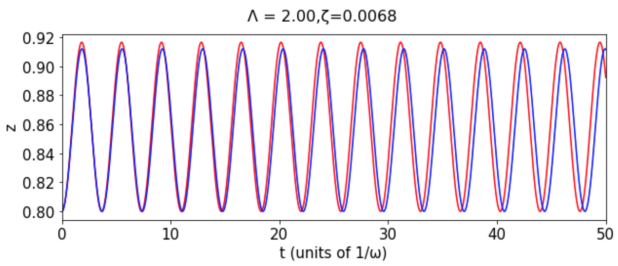

FIG. 1: Population imbalance as a function of time with initial values $z_0 = 0.8$ and $\delta\phi_0 = \pi$, for $\Lambda_0 = 2.00$. S2M results (red) and I2M results (blue). We have used the same parameters as in [6].

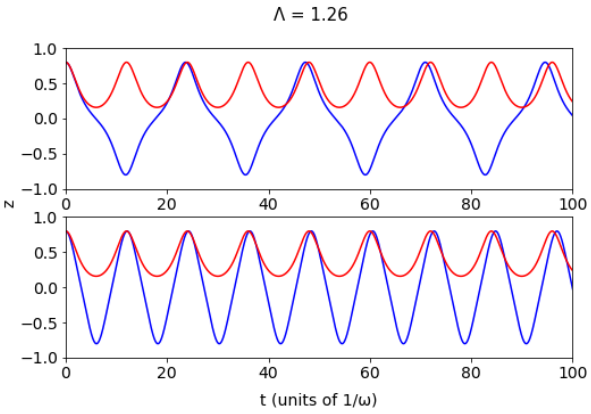

FIG. 2: Population imbalance as a function of time, $z_0 = 0.8$ and $\delta\phi_0 = \pi$, for $\Lambda_0 = 1.26$. S2M results (red) and I2M results (blue). The panel above represents the parameters from [6], the panel below from [9].

From Fig. 2 it is noticeable that for $\Lambda_0 = 1.26$, the S2M and I2M lead to two completely different behaviours. In this interaction regime, $\Lambda_0 \in [\Lambda_c, \tilde{\Lambda}_c]$, one should include the nonlinear interaction terms for a more accurate description of the transition between the two dynamical regimes.

Regardless of the value of ζ, both panels in Fig. 2 give rise to the same qualitative results. For the S2M, one can observe periodic oscillations around a population imbalance different from zero. Moreover, the sign of z does not vary over time. These features are characteristic of the MQST regime. On the other hand, when studying the I2M, one can observe that for the same interaction parameter and initial conditions as in the S2M, the periodic oscillations occur around $z = 0$, meaning that when averaged over time $\langle z \rangle_t = 0$. The dominant regime corresponds, in this case, to JE. Consequently, one can say that in the studied region of Λ_0, the suppression of tunneling happens for a higher Λ_0 for the I2M than in the S2M. In other words, the range of JE increases when the effects of the overlap are not neglected.

The results shown in Figs. 1 and 2, are in remarkable qualitative accordance with the behaviours from the two-mode approximations studied in Ref. [8].

B. Stability comparison between S2M and I2M

In this section we study the classical energy surfaces of the system, in the $(z, \delta\phi)$ plane, from Eqs. (13-14). Firstly, it is necessary to find the stationary points of the system in both approximations. Then, using the Hessian matrix, the stability of the stationary points can be studied.

We only consider repulsive interactions, Λ, $\tilde{\Lambda} > 0$. The stationary points resulting from the S2M approximation (13), are: $(z_0, \delta\phi_0) = \{(0,0), (0, \pm\pi), (\pm\mathcal{A}, \pm\pi)\}$, with $\mathcal{A} = \sqrt{1 - \Lambda^{-2}}$. We have studied the stability of these stationary points, summarized in Table I.

$(z_0,\delta\phi_0)$	Stationary	Minimum	Saddle	Maximum
(0,0)	$\forall\Lambda$	$\forall\Lambda$	—	—
(0,±π)	$\forall\Lambda$	—	$\Lambda > 1$	$\Lambda < 1$
(±$\mathcal{A}$,±π)	$\Lambda > 1$	—	—	$\Lambda > 1$

TABLE I: Stationary points and stability of the system depending on the value Λ in the S2M approximation.

On the other hand, the stationary points resulting from the I2M approximation (14), are the following: $(z_0, \delta\phi_0) = \{(0,0), (0, \pm\pi), (\pm\mathcal{B}, \pm\pi)\}$, where $\mathcal{B} = \sqrt{1 - (\tilde{\Lambda} - 3\zeta)^{-2}}$. In Table II we have studied the stability of these stationary points for $\zeta = 0.06$ [9].

$(z_0,\delta\phi_0)$	Stationary	Minimum	Saddle	Maximum
(0,0)	$\forall\tilde{\Lambda}$	$\forall\tilde{\Lambda}$	—	—
(0,±π)	$\forall\tilde{\Lambda}$	—	$\tilde{\Lambda} > 1.18$	$\tilde{\Lambda} < 1.18$
(±$\mathcal{B}$,±π)	$\tilde{\Lambda} > 1.18$	—	—	$\tilde{\Lambda} > 1.18$

TABLE II: Stationary points and stability of the system depending on the value $\tilde{\Lambda}$ in the I2M approximation.

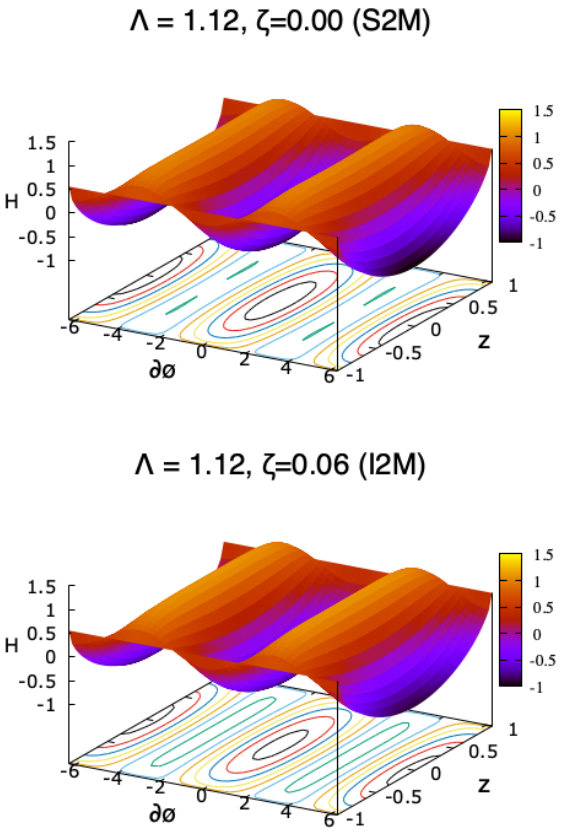

FIG. 3: Energy surfaces for $\Lambda = \tilde{\Lambda} = 1.12$. The lines on the $(z, \delta\phi)$ plane describe constant energy trajectories. Top panel corresponds to the S2M approximation, and bottom to the I2M, with the parameters from [9].

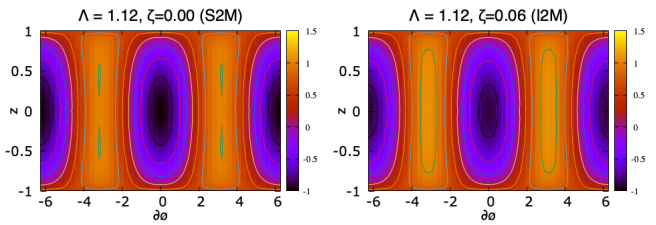

FIG. 4: Map of the energy surfaces for $\Lambda = \tilde{\Lambda} = 1.12$. Left panel: S2M approximation, and right panel: I2M, with the parameters from [9]. The lines represent trajectories of constant energy.

From Tables I and II, it is worth noticing that the stationary point $(z_0, \delta\phi_0) = (0, \pm\pi)$ has an inconclusive behaviour when $\Lambda = 1$ and $\tilde{\Lambda} = 1.18$, respectively.

The system, around either a maximum or a minimum, allows for closed orbits around that stationary point. However, when the stationary point is a saddle point, the system can no longer follow a closed orbit around it. Hence, JE can only be observed around a maximum or a minimum, together with the condition $\langle z \rangle_t = 0$. For the MQST regime, the situation is more complex. There are two different types of MQST depending of the evolution of the phase difference, $\delta\phi$. If the phase difference evolves bounded in time, the MQST is called either the *zero-mode* or π*-mode*, when $\delta\phi_0 = 0, \pm\pi$, respectively. In our study the *zero-mode* cannot be observed since it is exclusive for attractive interactions [7]. These modes are represented by closed orbits around the maximum or minimum. Contrarily, when the phase difference evolves unbounded, increasing or decreasing in time, one can observe orbits that are not closed. These kind of trajectories correspond to the so-called *running phase mode*.

Figs. 3 and 4, show that around $\delta\phi = \pm\pi$, only in the I2M approximation $\langle z \rangle_t = 0$, which means that the system still exhibits Josephson oscillations. However, when studying the S2M approximation, the closed orbits around $\delta\phi = \pm\pi$ are not centered in $z = 0$, meaning that $\langle z \rangle_t \neq 0$. This feature, as we have already mentioned, corresponds to MQST, specifically a π*-mode* MQST. The *running phase mode* is not observable for the initial conditions and interaction parameters used in our study. Nevertheless, keeping the same initial conditions, and increasing $\Lambda(\tilde{\Lambda})$, this mode would appear in both Figs. 3 and 4.

IV. CONCLUSIONS

In this work, we have studied the tunneling dynamics between two weakly-linked BECs. By using the two mode approximation, S2M and I2M, we have analyzed the importance of the overlap of the right and left wave functions. The numerical results, for both the temporal evolution of the population imbalance, and the stability of our system, lead to the conclusion that the I2M is indeed necessary when working in the range of critical values of the interaction parameters, $\Lambda_0 \in [\Lambda_c, \tilde{\Lambda}_c]$. In this range, the transition between the two dynamical regimes occurs. In the I2M, tunneling is supported in a wider range of interaction values, hence, the range where JE dominates is increased. One could expect this result, since for bosons, tunneling from the left to the right well, or vice-versa, is favoured when the effects of the overlap of the condensates wave functions are not neglected. For values of $\Lambda_0 \notin [\Lambda_c, \tilde{\Lambda}_c]$, the S2M yields similar results to the I2M. Accordingly, it would not be necessary to use the I2M outside that range.

Further work in this direction could be to numerically solve the GP equation, for example using the Crank-Nicolson method. This would allow to compare the results for a broader set of initial conditions and interaction parameters. Additionally, one could study how the system behaves when the condensates are not identical, the most common case is a binary mixture.

Acknowledgments

I would like to thank my advisor Dra. Montserrat Guilleumas for the help and encouragement throughout every step of the project.

I would also like to thank my family and friends for their unconditional support.

[1] E.A. Cornell, *Very Cold Indeed: The Nanokelvin Physics of Bose-Einstein Condensation*, J. Res. Natl. Stand. Technol., **101**, 419 (1996).

[2] L. Pitaevskii and S. Stringari, *Bose-Einstein Condensation*. Clarendon Press, Oxford (2003).

[3] J. F. Annet, *Superconductivity, Superfluids and Condensates*. Oxford University Press, Oxford (2004).

[4] M. Albiez et al., *Direct Observation of Tunneling and Nonlinear Self-Trapping in a Single Bosonic Josephson Junction*, Phys. Rev. Lett. **95**, 010402 (2005).

[5] A. Smerzi et al., *Quantum Coherent Atomic Tunneling between Two Trapped Bose-Einstein Condensates*, Phys. Rev. Lett. **79**, 4950 (1997).

[6] D. M. Jezek, P. Capuzzi, and H. M. Cataldo, *Two-mode effective interaction in a double-well condensate*, Phys. Rev. A **87**, 053625 (2013).

[7] M. Melé-Messeguer, B. Juliá-Díaz, M, Guilleumas, A. Polls, and A. Sanpera, *Weakly linked binary mixtures of F=1 ^{87}Rb Bose–Einstein condensates*. New J. Phys. **13**, 033012 (2011).

[8] D. Ananikian and T. Bergeman, *Gross-pitaevskii equation for Bose particles in a double-well potential: Two-mode models and beyond*, Phys. Rev. A **73**, 013604 (2006).

[9] M. Nigro et al., *Effective two-mode model in Bose-Einstein condensates versus Gross-Pitaevskii simulations*, Eur. Phys. J. D **71**, 297 (2017).